Institute of Mathematical Sciences

MAGNETO-FLUID DYNAMICS DIVISION

MF-24 NYO-9763

THE DEVELOPMENT OF COMPRESSION WAVES IN AN ADIABATIC TWO-FLUID MODEL OF A COLLISION-FREE PLASMA

K. W. Morton

June 30, 1961

AEC Research and Development Report

NEW YORK UNIVERSITY

UNCLASSIFIED

Magneto-Fluid Dynamics Division
Institute of Mathematical Sciences
New York University

Physics and
Mathematics

MF-24 NYO-9763

THE DEVELOPMENT OF COMPRESSION WAVES IN AN ADIABATIC TWO-FLUID MODEL OF A COLLISION-FREE PLASMA

K. W. Morton

June 30, 1961

AEC Research and Development Report

Contract No. AT(30-1)-1480

UNCLASSIFIED

ABSTRACT

A generalized discontinuous solution is found for the adiabatic two-fluid equations in the steady state: it covers the case of strong shocks and enables one to give a complete account of the steady state solutions of these equations. By considering a piston problem using numerical methods, time dependent solutions of the equations are also found; these rapidly steepen and converge to the discontinuous steady state solutions whenever these exist.

Table of Contents

The Development of Compression Waves in an Adiabatic Two-Fluid Model of a Collision-Free Plasma*

1. Introduction and Summary

The two-fluid model of a collision-free plasma has received considerable attention, especially the case of zero temperature where it coincides with the particle picture. Some steady state solutions are well-known(1)(2) and Gardner and Morikawa(3) have obtained an asymptotic solution for small amplitude waves. The simplest extension of the model to warm plasmas is the introduction of an adiabatic pressure and it has been suggested that this might provide a first approximation to a description of a collision-free shock (see Gardner, et al.(4) and Morawetz(5)). Baños and Vernon(6) and Vernon(7) have studied solitary wave and periodic steady state solutions of these equations and Gardner and Morikawa's asymptotic treatment can similarly be extended to this case. Our chief concern in this report is to study the development of a large amplitude compression wave by using numerical methods and to relate the situations holding after long intervals of time with the steady state solutions. Similar work using a different approach was briefly reported by Kilb, Auer and Hurwitz in 1960(8)(9) and is now fully described in references (13) and (14).

*This work was carried at the Institute of Mathematical Sciences while the author was on sabbatical leave from the United Kingdom Atomic Energy Authority, Harwell.

The specific problem that is studied here is the following: we have a half space of plasma at rest and with uniform density, bounded by a plane perfectly conducting piston, and containing a constant magnetic field parallel to the plane of the piston. The piston is now accelerated into the plasma to a final velocity at which it is held hereafter. The problem is to find the ensuing motion of the plasma and the changes in the magnetic field. Initially we asked the particular question - does the wave always break as in conventional non-dissipative fluid dynamics? Having found that in many cases this does occur, we have continuied the solution beyond this point using the von Neumann-Richtmyer artificial viscosity to integrate through the discontinuity that develops.

The first result, provoked by the behavior of the numerical solutions, is that "for sufficiently strong shocks" there exists a generalized solution of the steady state equations that is discontinuous in the fluid variable. This is described in Section 3 which contains a complete account of the steady state solutions. Briefly, there are always two constant states and the types of solution that exist depend on the compression ratio η between the states and the ratio β_o of the fluid to magnetic pressure in the initial state. The (η,β_o) plane is divided into three main regions --(i) for small η the solitary wave and, except for very small β_o, all the associated periodic waves exist; (ii) the solitary wave ceases to exist when, at its peak, the flow speed exceeds the characteristic speed and then only some of the periodic waves exist; and (iii) when

the characteristic speed exceeds the flow speed in the second constant state, the discontinuous solution appears. The two constant states have different entropies and only in case (iii) can they be joined by a solution.

The numerical solutions of the time dependent equations show a very close relationship to the steady state solutions: in case (iii) the convergence to the steady state solution is very rapid; and in case (ii), although convergence is not so rapid, a very close identification can be made between the actual solution and one composed from the steady state solutions. This solution consists of a partly discontinuous leading edge followed by a wave train, the first waves of which are the largest periodic solutions that exist in the particular case. In case (i) the leading edge appears to be no longer discontinuous and no such identification has been found possible.

The author wishes to thank C. S. Morawetz and J. Berkowitz for suggesting the problem and for many valuable discussions.

2. The Equations of Motion

We will take the piston to lie in the (y,z) plane and let it be moved in the positive x-direction; then all quantities depend only on x and the time t. We shall also confine ourselves to the case where the magnetic field remains in the z-direction*. The only electromagnetic quantities that will therefore arise in our equations are:

B the z-component of the magnetic field;

E the y-component of the electric field;

and J the y-component of the current.

Since there are no currents or electric fields initially, all other components are zero except for the x-component of of the electric field, the charge separation field, which will not enter.

Under these conditions the motion of the ions and electrons is essentially two-dimensional and the fluid equations can easily be derived from the collision-free Boltzmann equations for the two particles by taking moments of their distribution functions in the usual way. Further assumptions that are made in this derivation are that:

(i) there is charge neutrality -- except in Poisson's equation which is not needed;

and (ii) the pressure tensors of the ions and electrons

---

*Recent work by C. S. Gardner has shown that there is a much wider class of solutions when this restriction is relaxed.

are diagonal and together yield a total pressure that is isotropic in the (x,y) plane and satisfies a perfect gas law with adiabatic exponent $\gamma = 2$.

Thus we obtain the following conservation equations where we use subscripts to denote partial differentiation:

$$\rho_t + (\rho u)_x = 0 \tag{2.1}$$

$$\rho(u_t + u\, u_x) + p_x = JB \tag{2.2}$$

$$\overline{e}_t + [u(\overline{e} + p)]_x = JE \tag{2.3}$$

where

$\rho = \rho_+ + \rho_-$, the total mass density of ions and electrons;

$u = u_+ = u_-$, the common x-component of velocity;

and $\overline{e}$, the total internal energy density, may be written in the form

$$\overline{e} = p + \frac{1}{2}\rho u^2 + \frac{1}{2}\left(-\frac{m_+ m_-}{e_+ e_-}\right)\frac{J^2}{\rho} \tag{2.4}$$

m_+ , m_- and e_+ , e_- being the ion and electron masses and charges.

From the equations for the conservation of momentum in the y-direction we obtain an equation for the current:

$$J_t + (uJ)_x = \left(-\frac{e_+ e_-}{m_+ m_-}\right)\rho(E-uB) \tag{2.5}$$

And finally we have two of Maxwell's equations (we use rationalized m.k.s. units and neglect the displacement current):

(2.6) $\quad B_t + E_x = 0$ and $B_x + \mu J = 0$

where μ is the magnetic permeability of space.

The initial constant state is described by the three quantities ρ_o, p_o, and B_o, the initial values of ρ, p and B; and three functions of these quantities are of particular significance:

$$a_o = \frac{B_o}{(\mu\rho_o)^{1/2}}$$, the initial Alfvén speed;

$$\beta_o = \frac{p_o}{(B_o^2/2\mu)}$$, the ratio of the initial fluid and magnetic pressures;

and $$x_o = \left(- \frac{e_+e_-}{m_+m_-} \mu\rho_o \right)^{1/2} = (\mu k\, \omega_p^2)^{-1/2}$$, which can be regarded as either the ratio of the speed of light $(\mu k)^{-1/2}$ to the plasma frequency ω_p, or as the geometric mean of the gyromagnetic radii of ions and electrons moving across the initial field with speed a_o.

Introducing first the difference velocity*

---

* In fact, the difference between the ion and electron velocities is
$$\left(- \frac{e_+e_-}{m_+m_-} \right)^{1/2} \left(\frac{m_+}{e_+} - \frac{m_-}{e_-} \right) v$$

$$(2.7) \qquad v = \left(-\frac{m_+ m_-}{e_+ e_-}\right)^{\frac{1}{2}} \frac{J}{\rho}$$

in place of the current, we normalize all our variables in terms of these fundamental quantities in the following way:

$$x : x_o \qquad t : x_o/a_o$$

$$u : a_o \qquad v = a_o$$

$$\rho : \rho_o \qquad B : B_o$$

$$p : B_o^2/\mu \qquad \bar{e} : B_o^2/\mu$$

$$E : a_o B_o$$

There will be no confusion if we now denote the normalized variables by the same symbols as before. Equation (2.5) becomes

$$(2.8) \qquad v_t + u\, v_x = E - uB$$

which on combination with (2.6) yields an equation for $B + v_x$ identical with the continuity equation for ρ : since these quantities are equal initially, they remain so. In addition we may substitute for the internal energy

$$(2.9) \qquad \bar{e} = \frac{1}{2}\rho(u^2 + v^2) + p$$

in the energy conservation equation, obtaining the usual relation that the entropy is constant along the particle paths. Thus our equations become:

$$(2.10) \qquad \rho_t + (u\rho)_x = 0$$

$$(2.11) \qquad u_t + uu_x + (1/\rho)p_x = vB$$

$$(2.12) \qquad A_t + uA_x = 0$$

$$(2.13) \qquad v_x = \rho - B$$

$$(2.14) \qquad \rho v + B_x = 0 \;;$$

where

$$(2.15) \qquad p = A\rho^2 \quad .$$

The initial conditions are now

$$(2.16) \qquad \begin{gathered} \rho = B = 1 \quad , \qquad A = p = \tfrac{1}{2}\beta_o \\ u = v = 0 \end{gathered}$$

The piston, whose velocity will be prescribed, we shall assume is a perfect conductor. Thus E will equal uB just inside the plasma and, from (2.8), the derivative of v along the piston path will be zero; our boundary conditions on the piston become

$$(2.17) \qquad u = u_p(t), \qquad v = 0 \; .$$

It will be noticed that when $\beta_o = 0$ these boundary conditions together with equation (2.11) will not allow the piston to be accelerated. For $\beta_o > 0$ a boundary layer will develop at the piston which will become increasingly severe as $\beta_o \longrightarrow 0$ and prevent us from computing the limiting case.

Equations (2.10) to (2.15) are mixed hyperbolic-parabolic, their characteristics being the usual characteristics forn non-dissipative fluid flow plus two parallel to the x-axis which are the limits of the characteristics of the electromagnetic wave equation as the speed of light tends to infinity. When the plasma is assumed perfectly conducting, by (2.8) the derivatives of v can be neglected, so that $\rho = B$ and the equations reduce to those of ordinary fluid dynamics with the "total" pressure $p + \frac{1}{2} B^2$.

Because of the relevance of this "one fluid" theory in at least parts of the flow one might expect compressive waves to steepen and possibly form discontinuities. The form of these is apparent from the equations: if ρ and B remain finite, then by (2.17) so will v_x; thus there can be no jump in B or in v at the discontinuity, which will involve only the fluid quantities ρ, u, and p . The situation is then different from that in the one-fluid theory so perhaps one should not always expect continued steepening to the point of breaking. The jump conditions at any discontinuity that does arise, however, will be just the Rankine-Hugoniot relations in the usual fluid variables. This does not mean of course that the

shock that this might correspond to in a more accurate model would necessarily be an ordinary viscous shock.

3. Steady State Solutions of the Equations

In this section we shall consider solutions of the equations (2.10) to (2.15) which are steady when viewed from a frame of reference moving with a constant velocity U, the "shock" velocity. The existence of solitary wave and periodic solutions has been demonstrated previously for both cold and warm plasmas[1,2,6,7]. However, we cannot expect these to completely describe the situation in our problem long after the piston has attained its final velocity, for they do not satisfy all the boundary conditions; indeed, there cannot be any continuous steady state solution of these non-dissipative equations joining initial and final states with differing entropies. Thus we shall need to look for both continuous and discontinuous solutions; we shall see later that both play roles in the behavior of our system so we shall try to give a complete description of all solutions in this section.

Attaching primes to quantities referred to the moving frame of reference, the conservation equations become on integration

$$(3.1) \qquad \rho u' = -U$$

$$(3.2) \qquad -Uu' + p + 1/2\, B^2 = U^2 + 1/2\, \beta_o + 1/2$$

and

$$(3.3) \qquad -u'(\bar{e}' + p) + UB = U\beta_o + \frac{1}{2} U^3 + U$$

where the constants of integration have been determined from the initial state; in the last equation we have used the deduction from (2.6) that $E' = E - UB = \text{constant} = - U$. Now we replace the density ρ by the specific volume $V = \frac{1}{\rho}$ and substitute into (3.3) the expressions for u' obtained from (3.1), for p from (3.2), and for $\bar{e}'$ from (2.9); the result is a quadratic for V in terms of B and v :

$$(3.4) \quad 3U^2V^2 - 2V[2U^2 + 1 + \beta_o - B^2] + [U^2 - v^2 - 2B + 2 + 2\beta_o] = 0$$

The remaining equations (2.13) and (2.14) become

$$(3.5) \qquad V \frac{dv}{dx} + BV - 1 = 0$$

and

$$(3.6) \qquad V \frac{dB}{dx} + v = 0 .$$

Thus solutions are described by this pair of equations for B and v with V defined by one of the roots of (3.4). Constant states correspond to singularities of the differential equations, given by $v_i = 0$, $B_iV_i = 1$. If we substitute $1/B$ for V in (3.4) with $v = 0$, we find one root corresponding to the initial state $B_o = V_o = 1$, and the other, $B_1 = \eta = 1/V_1$, which we would like to identify with

a final state and for which

$$(3.7) \qquad U^2 = \frac{2(1+\beta_o)\eta}{3-\eta}$$

Clearly, when the compression ratio η is greater than unity, the shock velocity U is greater than the magneto-sonic speed $(1 + \beta_o)^{1/2}$.

The solutions are most conveniently described in the (B,v) plane; with these co-ordinates, equations (3.5) and (3.6) define a direction field on a two-sheeted surface, each sheet corresponding to a root of the quadratic (3.4) for V . The two sheets are joined on a closed convex curve on which these two roots are equal. Inside the curve the roots become complex so that no physically admissible solution may cross into this region. If we write the equation for the curve in the form

$$(3.8) \qquad \left\{B^2 - \frac{3(1+\beta_o)(\eta-1)}{3-\eta}\right\}^2 - \frac{12(1+\beta_o)B(B-\eta)}{3-\eta} + 3U^2v^2 = 0$$

we see that it always lies to the right of the second singularity $(B_1 = \eta,\ v_1 = 0)$; it passes through this point for the particular value of η given by

$$(3.9) \qquad \frac{3(\eta-1)}{\eta^2(3-\eta)} = \frac{1}{1+\beta_o} \quad .$$

Two other physical conditions may further confine the position of solutions on the two sheets: firstly, the entropy cannot fall below its initial value, i.e., $A \geq \beta_o/2$; and secondly

the density must remain positive, i.e., $V \geq 0$. However, when p is replaced by A/V^2 the momentum equation (3.2) can be written as a cubic for V,

$$V^3 + V^2 \left\{ \frac{B^2 - 1 - \beta_o}{2U^2} - 1 \right\} + \frac{A}{U^2} = 0 \tag{3.10}$$

the two positive (or complex) roots of this being those of (3.4). Thus only when $A = \beta_o = 0$ does V become zero and then the two roots become zero together so that the condition that we remain outside (3.8) already contains this restriction.

Now let us turn to the nature and position of the singularities. The discriminant for the characteristic equation takes on the simple form $V^{-2}\partial(VB)/\partial B$ at the singularities, which on computing the derivative becomes

$$\Delta_i = \frac{M_i^2 - 1 - \beta_i}{V_i(M_i^2 - \beta_i)}, \qquad (i = 0, 1) . \tag{3.11}$$

Here

$M_i^2 = u_i'^2 \rho_i \; B_i^2 = V_i^3 U^2$, the square of the Alfven Mach number, and

$\beta_i = 2p_i \; B_i^2$, the ratio of the fluid to the magnetic pressure. At the initial state $M_o^2 = U^2 \geq 1 + \beta_o$ for $\eta \geq 1$ so that this singularity is always a saddle point in the cases we are interested in. It is also easily ascertained that it always lies on the sheet corresponding to the larger of the roots for V. At the second singularity M_1^2 is always less than $1 + \beta_1$ so that the singularity is a center if $M_1^2 > \beta_1$

and a saddle point if $M_1^2 < \beta_1$. This condition can be written in the form

$$(3.12) \qquad \frac{3(\eta-1)}{\eta^2(3-\eta)} > \frac{1}{1+\beta_o} \quad .$$

If η is so small that the condition is not satisfied then the singularity is a center and also it lies on the sheet of the larger root; if (3.12) is satisfied then it is a saddle point and it lies on the sheet of the smaller root. The changeover occurs when η satisfies (3.9) when, as we have already seen, both sheets contain the singularity. Thus a solution can always leave the initial state on the sheet of the larger root but only when (3.12) is satisfied can it enter a final state and this is on the other sheet. To make the change from one sheet to the other there must be a discontinuity in V , which will occur where the two solutions issuing from the end states meet in the (B,v) plane. This is what was expected from the time dependent equations. It is worth noting that to obtain a change from one sheet to the other which is continuous in V would involve both solutions being tangential to the curve (3.8); this does not occur in general, but one particular case is of interest as we shall see in the next section.

We are now in a position to tie all these observations together in a complete description of the three main types of steady state solution. For any given value of $\beta_o (0 \leq \beta_o \leq \infty)$ the situation depends on one other parameter, either U or η which are connected by equation (3.7); we shall use the latter

which lies in the range $(1 \leq \eta \leq 3)$, and the domains in which each situation holds are shown in Figure 1. For sufficiently weak disturbances, i.e., η near unity, a solitary wave solution exists and appears as a lobe in the (B,v) plane about the center at $B_1 = \eta$, $v_1 = 0$; inside this is a complete set of periodic solutions of increasing entropy and decreasing amplitude as they circle nearer and nearer to the center. This situation (which is illustrated by two of the cases shown in Figure 2) holds because either the domain D_V, in which the roots of (3.4) are complex, is empty or it lies to the right of the solitary wave lobe. D_V is empty in the region above and to the left of curve C_1 in Figure 1; on this curve it appears as a single point which for $\beta_o > 0.03704$ (or $\eta < 1.6$) is outside the solitary wave, while otherwise it is inside. In this latter case, as η is increased D_V expands excluding more and more of the periodic solutions until it intersects the solitary wave lobe; this region is shown as a small triangle bounded by curves C_1, C_2 and the line $\beta_o = 0$ in Figure 1. For the larges values of β_o the domain D_V approaches the solitary wave lobe from the outside; in both cases intersection occurs on the curve C_2 given by

$$(3.13) \qquad \frac{2(2-\eta)^3}{\eta^2(3-\eta)} = \frac{\beta_o}{1+\beta_o}$$

and beyond this the solitary wave no longer exists. Both the solitary wave and the periodic solutions lie entirely on the sheet corresponding to the larger root for V. The other sheet

contains no singularities and its solutions consist of a series of curves, each crossing the B-axis at just one point and curving to the left.

As η increases beyond the value given by (3.13), the domain D_V approaches the second singularity (B_1, v_1), excluding more and more periodic solutions, until on curve C_3 its boundary passes through it. Beyond this point (B_1, v_1) is a saddle point on the second sheet In this case, illustrated by the last diagram of Figure 2, there are two particularly interesting solution curves, one issuing from the first singularity on one sheet with positive dv/dB, and one from the second on the other sheet with a negative dv/dB; they meet at a point on the (B,v) plane where a jump discontinuity in V joins them. Plotted against the Lagrangian space co-ordinate they will appear as in Figure 7. This is the only steady state solution that joins two distinct constant states.

The above description has been almost entirely mathematical but the physical meaning of the restrictions placed on each type of solution can now be made clear. The gas sound speed, which is also the characteristic speed is $(2pV)^{1/2}$ and in the constant states equals $(\beta_i B_i)^{1/2}$; also the flow speed is $u_i' = M_i B_i^{1/2}$. Thus the condition $M_1^2 < \beta_1$ for the discontinuous solution to exist is merely the usual shock condition, that the flow behind the shock be subsonic, applied at the constant state. That there is such a gap before this solution exists is partly due to the role played by the one-fluid model, in which

the characteristic speed is $[(1+\beta_i)B_i]^{1/2}$. In the two constant states, $BV = 1$ and $v = 0$ and the conservation equations (3.1) to (3.3) applied to these states reduce to the Rankine-Hugoniot conditions for the one fluid model with a total pressure $p + \frac{1}{2} B^2$ and total energy $\bar{e} + \frac{1}{2} B^2 V$. In particular, equation (3.7) for the shock speed corresponds to Prandt's shock relation

$$(3.14) \qquad \mu^2 u_o'^2 + (1-\mu^2)c_o^2 = u_o' u_1'$$

where $\mu^2 = \frac{1}{3}$ and $c_o^2 = 1+\beta_o$. Thus one arrives at the twin conditions for the existence of the discontinuous solution, $M_o^2 > 1+\beta_o$ and $M_1^2 < \beta_1$, which clearly leaves a gap in the range of values of η for which they can be satisfied.

In addition, Vernon[7] expresses the condition (3.13) for the limit of the domain in which the solitary wave exists, as

$$(3.15) \qquad V_m = \nu \qquad \text{where} \quad \nu^3 = \beta_o / U^2$$

and V_m is the value of V at the peak of the solitary wave. This condition can be written in the form $u' = VU = (\beta_o/V)^{1/2} = (2pV)^{1/2}$, i.e., that for an infinitely weak shock. We shall see in the next section that in the domain between curves C_2 and C_3 of Figure 1 discontinuities do occur even though they cannot directly link constant states.

4. Numerical Solution of the Time Dependent Equations

For the numerical calculations it is most convenient to work with the equations in their Lagrangian form. In addition, to enable the computations to be simply continued through the shock fronts we introduce a von Neumann-Richtmyer[10] artificial viscosity. The equations are then

$$u_t + \left[\frac{A}{V^2} + q + \left(\frac{\alpha}{2}\right)B^2\right] = 0 \tag{4.1}$$

$$V_t = u_x \tag{4.2}$$

$$A_t + (qV)V_t = 0 \quad \text{where} \begin{cases} qV = a^2h^2(u_x)^2 & \text{if} \quad u_x < 0 \\ qV = 0 & \text{if} \quad u_x \geq 0 \end{cases} \tag{4.3}$$

$$B_{xx} = BV - 1 \tag{4.4}$$

The parameter α, which is normally unity, enables us to make a simple transformation of the variables to deal with cases of very high β_o; and a^2 is a parameter used to control the amount of artificial viscosity introduced. The initial and boundary conditions are,

$$t = 0, \quad x \geq 0: \quad B = V = 1, \quad u = q = 0, \quad A = \beta_o/2 \tag{4.5}$$

$$t > 0, \quad x = 0: \quad B_x = 0, \quad u = u_P(t)\ . \tag{4.6}$$

The difference scheme used to approximate these equations is fully described in Appendix A; it allows explicit integration of the first three equations while (4.4) is solved implicitly; all differences are centered on a staggered mesh except for the expression for q_x in the first equation. Criteria for the stability of the difference scheme are effectively the same as those for pure fluid dynamics, there being one for the shocked region and one for the smooth flow outside this as described, for example, by Richtmyer[11]. A running check on the computation is provided by the energy conservation integral,

$$(4.7) \quad u_P[p + q + (\tfrac{\alpha}{2})B^2]_P = \frac{d}{dt}\int_0^\infty [\tfrac{1}{2} u^2 + pV) + \alpha(\tfrac{1}{2} B_x^2 + \tfrac{1}{2} B^2 V)]dx$$

where the suffix P is used to refer to qualities evaluated at the piston.

For illustrative purposes attention has been concentrated on five cases for each of which $\beta_0 = 0.1$; in each case the piston is accelerated uniformly from rest to a final velocity in either one or two units of time; it is then held at this velocity thereafter, the five cases corresponding to final velocities of 0.1, 0.4, 0.5, 1.0 and 1.5. After an initial period in which the effect of the acceleration is dominant, the solutions in general settle down to a fairly common form which consists of four portions. The disturbance propagates into the plasma at a more or less definite speed and with a leading edge that may steepen and break into a partly discontinuous form. This is followed by a wave train of

increasing length, the amplitude of the waves decreasing away from the disturbance front until a constant state is reached; the constant state makes up the third portion of the solution and extends almost to the piston to which it is joined by a narrow boundary layer. Figure 4 shows a typical example.

For at least three of the cases a detailed description of the results can be obtained by reference to the steady state solutions described in the previous section. The only difficulty arises in the identification of each case with a point in Figure 1, which determines what steady state solutions are available. The matching of β_0 is immediate and for the other parameter we have identified the final piston velocity with the fluid velocity in the second constant state and used the steady state equations to obtain η, U etc. Another possibility would be to measure the shock velocity U from the numerical results and use this as the starting point of the matching; but we prefer to attempt a complete prediction from given data even if this does have a greater error. Using the first method, then, the five cases correspond to the points marked with a cross in Figure 1 and the situation on the (B,v) plane for each case is shown in Figure 2.

As would be expected, case V is the most straightforward; a discontinuous steady state solution joining the initial state to the state corresponding to the piston velocity exists and our matching is therefore correct. The piston reached its final velocity at $t = 2.0$ and by $t = 12.5$ the front of the

wave looks as in Figure 7; the corresponding steady state solution is shown on the same figure. There is very close agreement except in a region one unit wide in which the artificial viscosity resolves the discontinuity in V. The shock speed and the state behind the front agree very well too, as can be seen from Table 1.

In case IV the wave train behind the discontinuity appears and in case III these waves are of increased amplitude and wavelength ; parts of the solutions (at $t = 20$ and $t = 40$, respectively) are shown in Figures 6 and 5. By this time the leading part of the solution has reached a steady form and the first wave of the following train is beginning to have a readily identifiable wavelength. Turning to the (B,v) diagrams in Figure 2, we can see how this form is made up from the steady state solutions. The second singularity is still on the sheet corresponding to the larger root for V and around it there is a set of periodic solutions, that with largest amplitude touching the boundary of the domain D_V at a point on the B axis. Also passing through this point and touching D_V is a solution on the other sheet, using the smaller root for V, which eventually intersects the curve corresponding to what is left of the solitary wave. Where these two solutions and the boundary of D_V touch is the only place where a solution may change from one sheet to the other without causing a discontinuity in V and A. Thus a solution can be made up of (i) an initial part along the solitary wave curve, (ii) a jump to the second sheet, (iii)

continuation on this sheet to the point of contact with the boundary of D_V on the B-axis, ending with (iv) the continuous traversal of the periodic solution loop. Solutions constructed in this way are shown for cases III and IV on Figures 5 and 6 below those obtained for the time dependent problem. There is a very considerable agreement even at this early stage in the development of the wave train and with the matching of parameters described above.

In Table 1 the shock velocities and the values of the variables in the constant state that develops near the piston are compared with those obtained from the steady state. As we should expect, the shock velocity and the characteristics of the wave train are consistent, their difference from the steady state values arising mainly from incorrect choice of the parameter η ; but the constant state cannot be properly compared with anything from the steady state solutions for its entropy is that of the largest periodic solution forming the head of the wave train, and not that of the constant state at the second singularity. Further, it is joined to the front of the disturbance by the time dependent part of the wave train.

The values of the parameters for case II suggest that a different type of solution may be obtained in which there are no discontinuities and the solitary wave plays a larger part. In fact, we have been unable to describe the solution in terms of the steady state solutions in either this case or in case I.

The development of the solution in case II is, however, rather interesting. This is illustrated by Figure 3 in which we have plotted the value of A at the first minumum in V (i.e., just behind what would be the shock) as a function of time. Apart from an early excursion near the time that the piston is being accelerated, A increases gradually, due to steepening of the front coupled with the artificial viscosity, until $t \sim 45$; it then rises sharply as the wave appears to break, reaching a maximum at $t = 60$; from here it decreases at a steady rate as the break weakens until from $t = 105$ to $t = 150$ it remains at a uniform level corresponding to a very steady leading edge of the wave. The whole of the wave train at $t = 60$ and the leading part at $t = 120$ are shown in Figure 4; the most significant measurable parameter seems to be the wavelength of the leading waves which remains at 10.7 from $t = 100$. No quantitative explanation of this has been found but the similarity of the problem with that of bores suggests that a treatment like that given by Benjamin and Lighthill[12] might be possible.

The low piston speed for case I was chosen with the hope that the behavior of the solution might approximate the asymptotic form given by Gardner and Morikawa[3] for a cold plasma. The equations that they give can also be derived for the present case and implies that $1-B$, $1-\rho$, and $u(1+\beta_o)^{-1/2}$ are all equal; moreover, in the particular solution they give the waves have a definite amplitude related to the piston velocity and widen with time like $t^{1/3}$. At $t = 100$ when the integration of case I was stopped the amplitude of the waves was still

growing although it was already much greater than that predicted. None of the other features were reproduced to a useful degree of approximation.

5. Discussion of the Results.

We have shown that, in the present model when the shock speed or compression is too great for the solitary wave to exist, there are still steady state solutions. These involve discontinuities at which entropy is lost and lead either to periodic waves with a distinctive form or, in the case of the greatest shock speeds, to a constant state. Moreover, in these cases the solution of the time dependent piston problem converges to these solutions.

The mechanism by which entropy is lost at the discontinuities is completely unspecified so that we have so far refrained from calling these phenomena collisionless shocks. The distance scale on which the discontinuity appears is the familiar geometric mean of ion and electron Larmor radii so its resolution demands a mechanism operating on a scale length related to either the electron Larmor radius or perhaps the Debye radius. It may be significant that on calculating the charge separation field from the solitary wave solution, Vernon[7] found that it became infinite where the solitary wave ceased to exist. To neglect this, as we have done, is clearly unjustified and should be the first thing included in a more detailed model of the shock structure.

Appendix A: Finite Difference Equations

Using a constant mesh size h and a time step k, let u be correctly centered at points $x = jh$, $t = (n - \frac{1}{2})jm$ $(j,h = 0,1,\ldots)$ and denote its value at these points by u_j^n; similarly let $V,B,$ and A be centered at $x = (j + \frac{1}{2})h$, $t = nk$, their values being denoted by V_j^n etc., finally qV and q will be centered at $x = (j + \frac{1}{2})h$, $t = n - \frac{1}{2})k$. We then have the difference equations

$$\text{(A.1)} \qquad u_{j+1}^{n+1} = u_{j+1}^{n} - \frac{k}{h}\left\{ \frac{A_{j+1}^{n}}{\left(V_{j+1}^{n}\right)^2} - \frac{A_j^n}{\left(V_j^n\right)^2} + q_{j+1}^{n} - q_j^n + \frac{\alpha}{2}\left[\left(B_{j+1}^{n}\right)^2 - B_j^{n}{}^{2}\right]\right\}$$

$$\text{(A.2)} \qquad V_j^{n+1} = V_j^n + \frac{k}{h}\left\{u_{j+1}^{n+1} - u_j^{n+1}\right\}$$

$$\text{(A.3)} \qquad A_j^{n+1} = A_j^n - (qV)_j^{n+1}\left(V_j^{n+1} - V_j^n\right)$$

where
$$(qV)_j^{n+1} = a^2\left\{u_{j+1}^{n+1} - u_j^{n+1}\right\}^2 \quad \text{if } \left\{u_{j+1}^{n+1} - u_j^{n+1}\right\} < 0$$
$$= 0 \quad \text{if } \left\{u_{j+1}^{n+1} - u_j^{n+1}\right\} \geq 0$$

$$\text{(A.4)} \qquad B_{j+1}^{n+1} - \left(2 + h^2 V_j^{n+1}\right)B_j^{n+1} + B_{j-1}^{n+1} = -h^2$$

and

$$(A.5) \qquad q_j^{n+1} = (qV)_j^{n+1} \left\{ \frac{2}{V_j^{n+1} + V_j^n} \right\}$$

These equations are solved in the order given. When solving (A.2), u_o^{n+1} is obtained from the expression for the piston velocity which is given; and (A.4) which is implicit needs boundary conditions at each end. At the piston we have $B_{-1}^{n+1} = B_o^{n+1}$ while the other boundary is allowed to move outwards by adding points until

$$B_{J+1}^{n+1} - 1.0 \leq \varepsilon$$

where ε is some prescribed error. Since V decays to its value at $x = +\infty$ more rapidly that B, $B-1.0$ has a tail of the form e^{-x} and we use this as the outer boundary condition. The tri-diagonal matrix equations for B are solved in the usual recurrence relation manner (see, for example, Richtmyer[11]). For the more accurate equations which we usually used

$$(A.6) \qquad (1 - \frac{h^2}{12} V_{j+1})B_{j+1} - (2 + \frac{5h^2}{6} V_j)B_j + (1 - \frac{h^2}{12} V_{j-1})B_{j-1} = - h^2$$

where we have dropped the superfixes, the procedure becomes:

$$E_1 = 1 \quad , \qquad F_1 = 0$$

$$(A.7)\qquad E_{j+1} = \frac{(1 - \frac{h^2}{12} V_{j+1})}{[(2 + 5h^2/6 \ \ V_j)-(1 - h^2/12 \ \ V_{j-1})E_j]} \quad ,$$

$$F_{j+1} = \frac{h^2 + (1 - \frac{h^2}{12} V_{j-1})F_j}{[(2 + 5h^2/6 \ V_j)-(1 - h^2/12 \ V_{j-1})E_j]}$$

$j = 1, 2, \ldots, J$

followed by

$$(A.8)\qquad B_{J+1} = \frac{F_{J+1} + \Gamma - 1}{\Gamma - E_{J+1}}$$

where $\Gamma = \left[1 + \frac{5h^2}{12} + h(1 + \frac{h^2}{6})^{1/2}\right] \Big/ (1 - \frac{h^2}{12})$

$$(A.9)\qquad B_j = F_{j+1} + E_{j+1} B_{j+1} \ ; \qquad j = J, J-1, \ldots, 0.$$

Stability. In regions of smooth flow away from shocks we may take $q = 0$. Then the amplification matrix for equations (A.1)-(A.3), (A.6) in terms of the variables u, V, and A is

$$
\text{(A.10)} \qquad \begin{pmatrix} 1 & 2id^2 & -2ig/V^2 \\ 2ig & 1-4g^2d^2 & 4g^2/V^3 \\ 0 & 0 & 1 \end{pmatrix}
$$

where $\quad g = (k/h) \sin \frac{1}{2} mh = (k/h)s$

and $\quad d^2 = \frac{2A}{V^3} + \alpha B^2 \quad \frac{h^2(1 - \frac{1}{3} s^2)}{4s^2 + h^2(1 - \frac{1}{2} s^2)V}$

$$= 2A/V^3 + O(h^2), \quad \text{normally.}$$

The corresponding characteristic equation is

$$
\text{(A.11)} \qquad (\lambda-1)[\lambda^2 - (2-4g^2d^2)\lambda + 1] = 0
$$

so that for the most practical purposes the stability condition is the usual one that $(h/k) > (2A/V^3)^{1/2}$, the sound speed (in Lagrangian coordinates).

In the shocked region the magnetic field and its first derivative are continuous so that in this narrow region the equations are identical to those of fluid dynamics: for these, Richtmyer(11) gives the condition:

$$\frac{k}{h}\left(\frac{2A}{V^3}\right)^{\frac{1}{2}} \leq \frac{[\eta(\eta - 1/3)]^{1/2}}{2a(\eta-1)}$$

where η is the shock stength, or compression ratio of the shock.

Table 1. Summary of the Cases Computed

$\beta_o = 0.1$ Limiting Solitary Wave occurs at $\eta = 1.4685$, $U = 1.4524$ at peak of which $V = 0.3619$.

Discontinuous Solution exists for $\eta > 2.1807$ $U > 2.4198$

	Case I	Case II	Case III	Case IV	Case V
Piston Speed	0.1	0.4	0.5	1.0	1.5
Steady State Solns.					
U	1.1265	1.3909	1.4888	2.0394	2.6631
(i) Constant State					
B_1	1.0974	1.4037	1.5056	1.9621	2.2897
V_1	0.9112	0.7124	0.6642	0.5096	0.4367
A_1	0.0502	0.0615	0.0710	0.1726	0.3668
(ii) Largest Periodic Soln.					
Wave Length	∞	∞	9.80	4.45	0
A	0.0500	0.0500	0.0563	0.1719	0.3668
Time Dependent Solns.	t=100	t=150	t=40	t=20	t=12.5
U	/	1.440	1.53	2.04	2.66
(i) Constant State					
u	0.1000	0.4000	0.5000	1.0000	1.50000
B	1.0998	1.419	1.530	1.970	2.291
V	0.909	0.705	0.653	0.508	0.4365
A	/	/	/	/	0.371
(ii) Wave Train Wavelength	/	10.7	8.8	4.0	/
A	0.500	0.0506	0.069	0.174	/

References

1. Adlam, J.H. and J.E. Allen, "The structure of steady collision-free hydromagnetic waves", Phil. Mag. 3, 448 (1958)

2 Davis, L., R. Lüst and A. Schlüter, "The structure of hydromagnetic shock waves. I. Non-linear hydromagnetic waves in a cold plasma", Z. Naturforsch. 13a, 916 (1958).

3. Gardner, C.S. and G. K. Morikawa, "Similarity in the Asymptotic Behavior of Collision-free Hydromagnetic Waves and Water Waves", TID-6184, Institute of Mathematical Sciences, New York University (1960).

4. Gardner, C. S., H. Goertzel, H. Grad, C. S. Morawetz, M. H. Rose, and H. Rubin, "Hydromagnetic Shock Waves in High Temperature Plasmas", Proc. of the Second U. N. International Conf. on the Peaceful Uses of Atomic Energy, vol. 31, 230 (1958).

5. Morawetz, C.S. "Magneto-hydrodynamic Shock Structure Using Friction", NYO-8677, Institute of Mathematical Sciences, New York University (1959).

6. Baños, Jr., A. and A. R. Vernon, "Large amplitude waves in a collision-free plasma. I. Single pulses with isotropic pressure", Nuovo Cimento XV, 269 (1960).

7. Vernon, A.R., "Large Amplitude Waves in a Collision-free Plasma", LRL-No. 3, University of California, Los Angeles (1960).

8. Kilb, R. W., and P.L. Auer, "Magnetic compression waves in a Collision-free Plasma", Bull. Am. Phys. Soc. II, 5, 353

(1960).

9. Auer, P. L., and H. Hurwitz, Jr., "Shock Relations in Magnetic Compression Waves", Bull. Am. Phys. Soc. II 5, 353 (1960).

10. von Neumann, J., and R. D. Richtmyer, "A Method for the Numerical Calculation of Hydrodynamic Shocks", J. Appl. Phys. 21, 232 (1950).

11. Richtmyer, R. D., Difference Methods for Initial Value Problems Interscience Publishers, New York (1957).

12. Benjamin, T. B., and M. J. Lighthill, "On Cnoidal Waves and Bores", Proc. Roy Soc. A 224, 448 (1954).

13. Auer, P. L., H. Hurwitz, Jr., and R. W. Kilb, "Large amplitude magnetic compression of a collision-free plasma. I Propagation of simple waves", General Electric Research Laboratory Report No. 61-RL-(2663 E), (1961).

14. Auer, P. L., H. Hurwitz, Jr., and R. W. Kilb, "Large amplitude magnetic compression of a collision-free plasma. II Development of a thermalised plasma", General Electric Research Laboratory Report No. 61-RL-(2758 E), (1961).

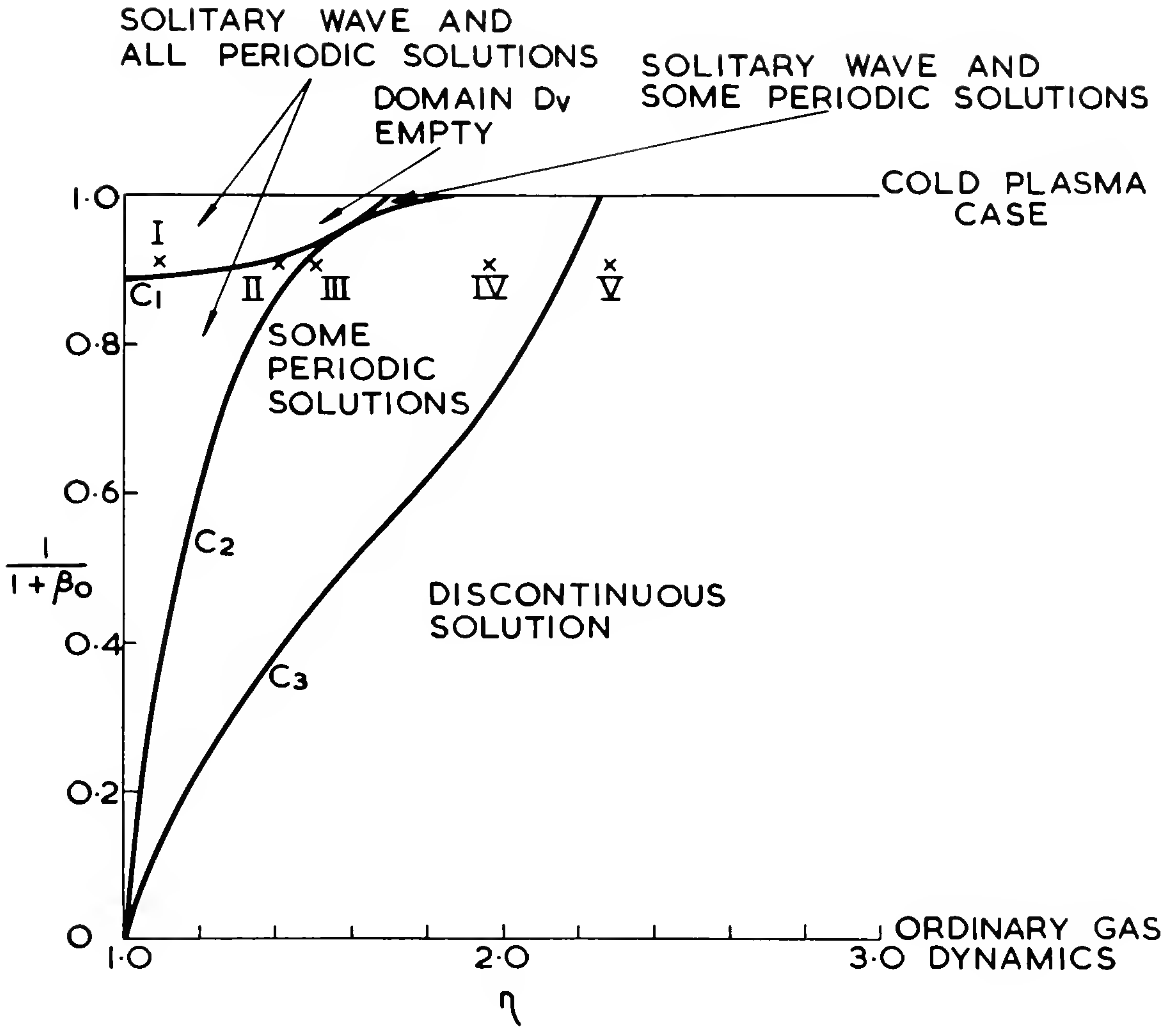

FIG. 1. DOMAINS OF EXISTENCE OF THE STEADY STATE SOLUTIONS AND THE POSITIONS OF CASES I TO V.

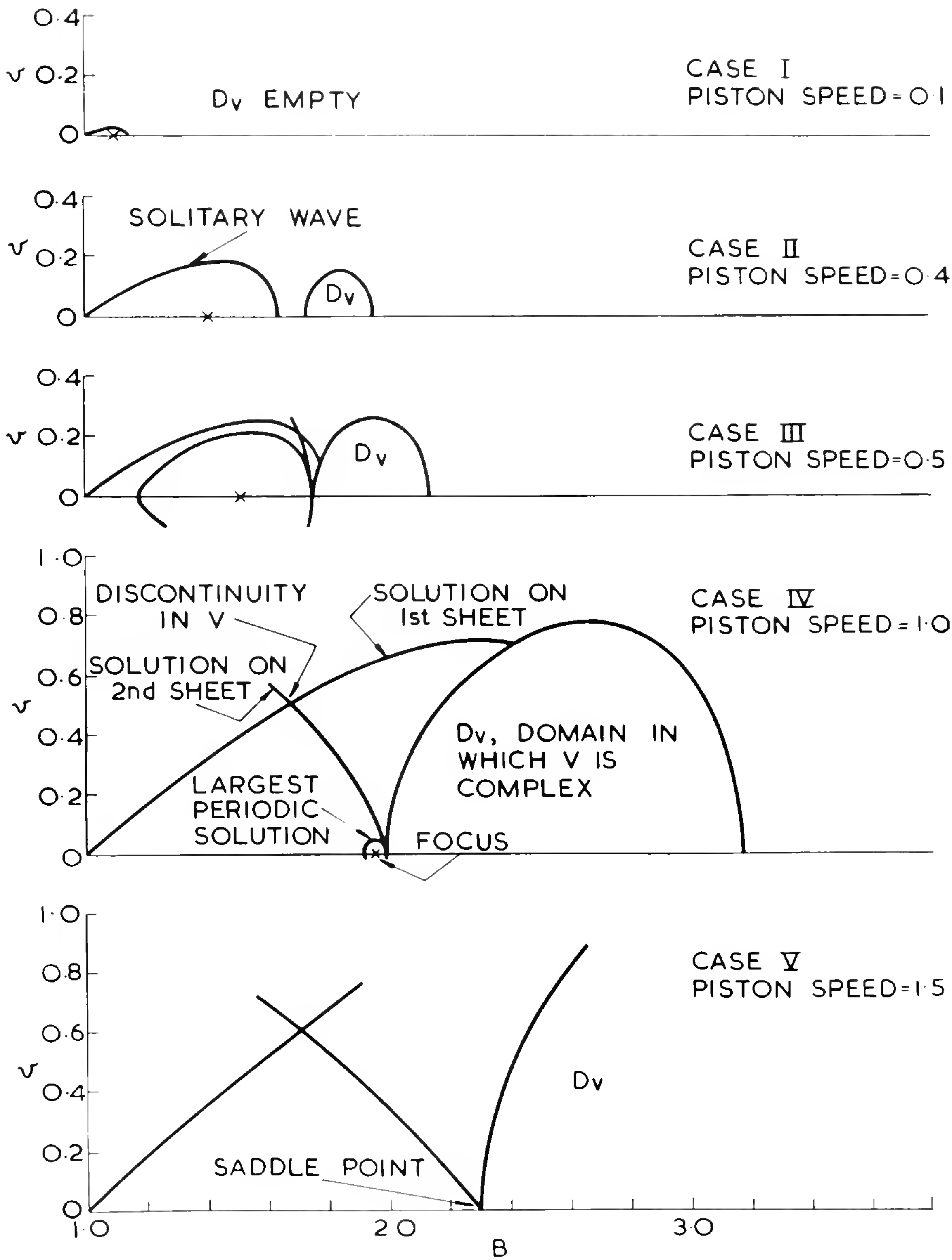

FIG 2. BEHAVIOUR OF THE STEADY STATE SOLUTIONS IN THE (B, v) PLANE

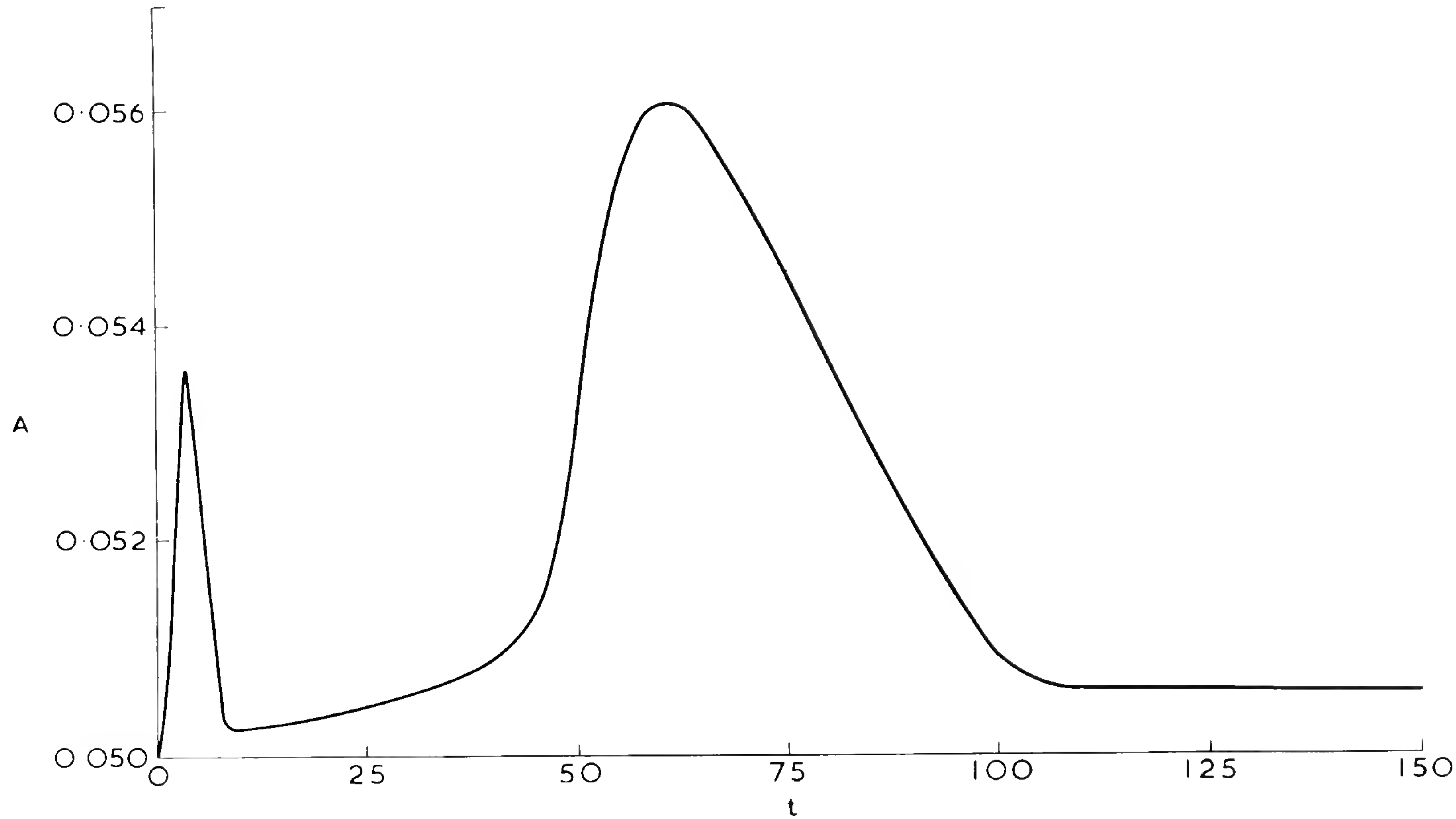

FIG 3. VARIATION OF THE VALUE OF A JUST BEHIND THE WAVE FRONT IN CASE II

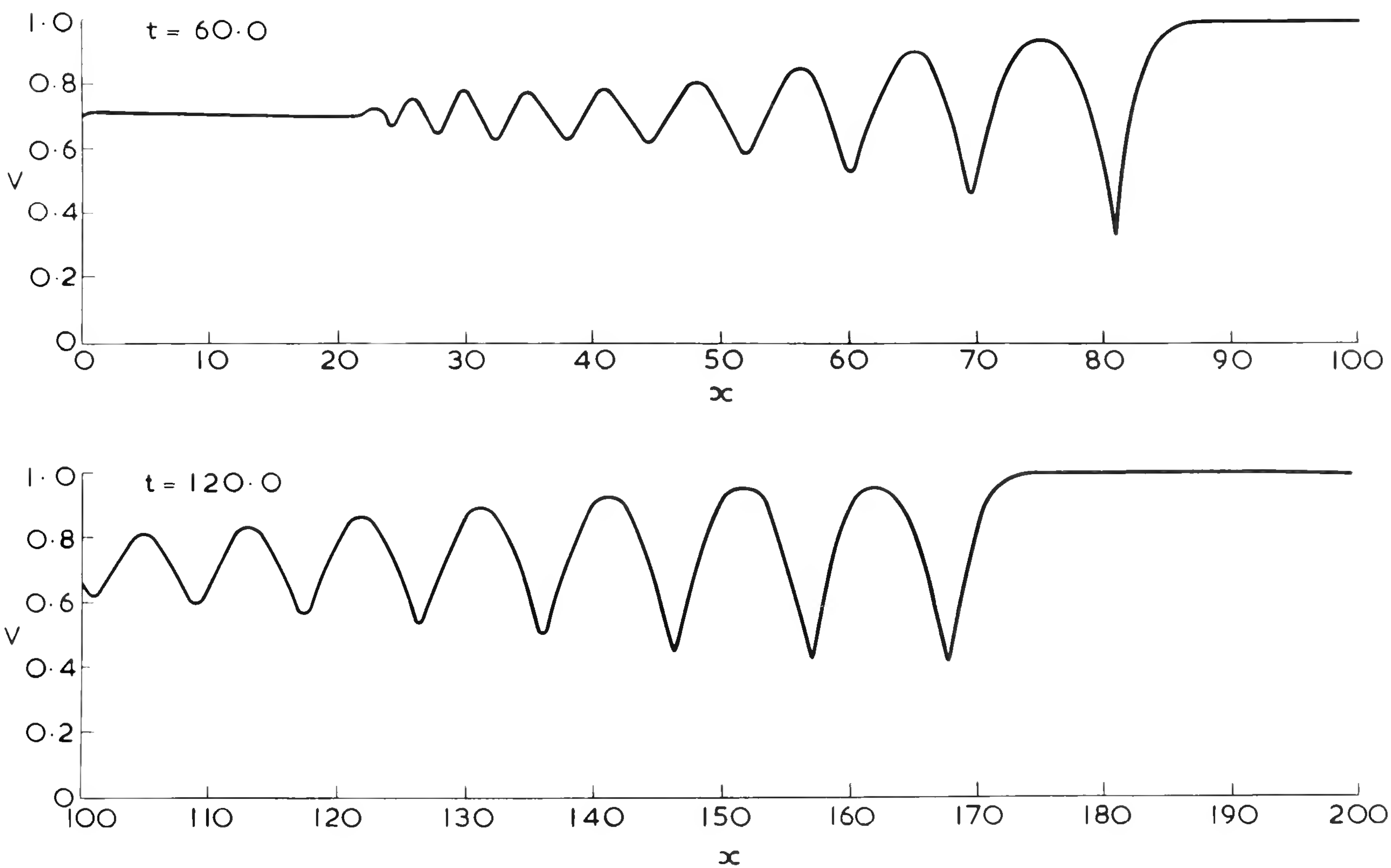

FIG 4 THE WAVE-FORM FOR V AT t = 60·0 AND 120·0 FOR CASE II ; x IS THE LAGRANGIAN CO-ORDINATE.

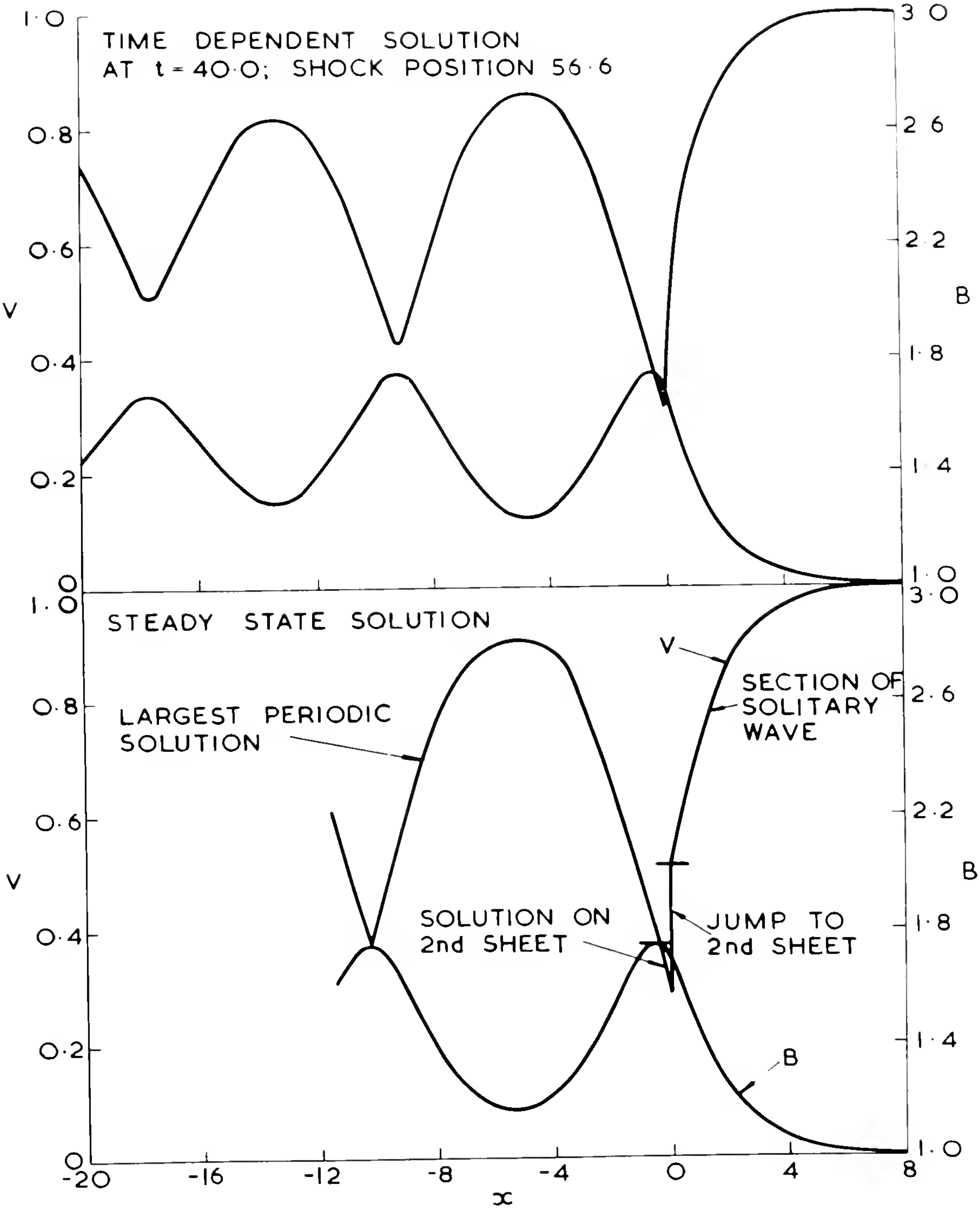

FIG. 5. COMPARISON OF THE TIME DEPENDENT SOLUTION AND A COMPOSITE STEADY STATE SOLUTION FOR CASE III.

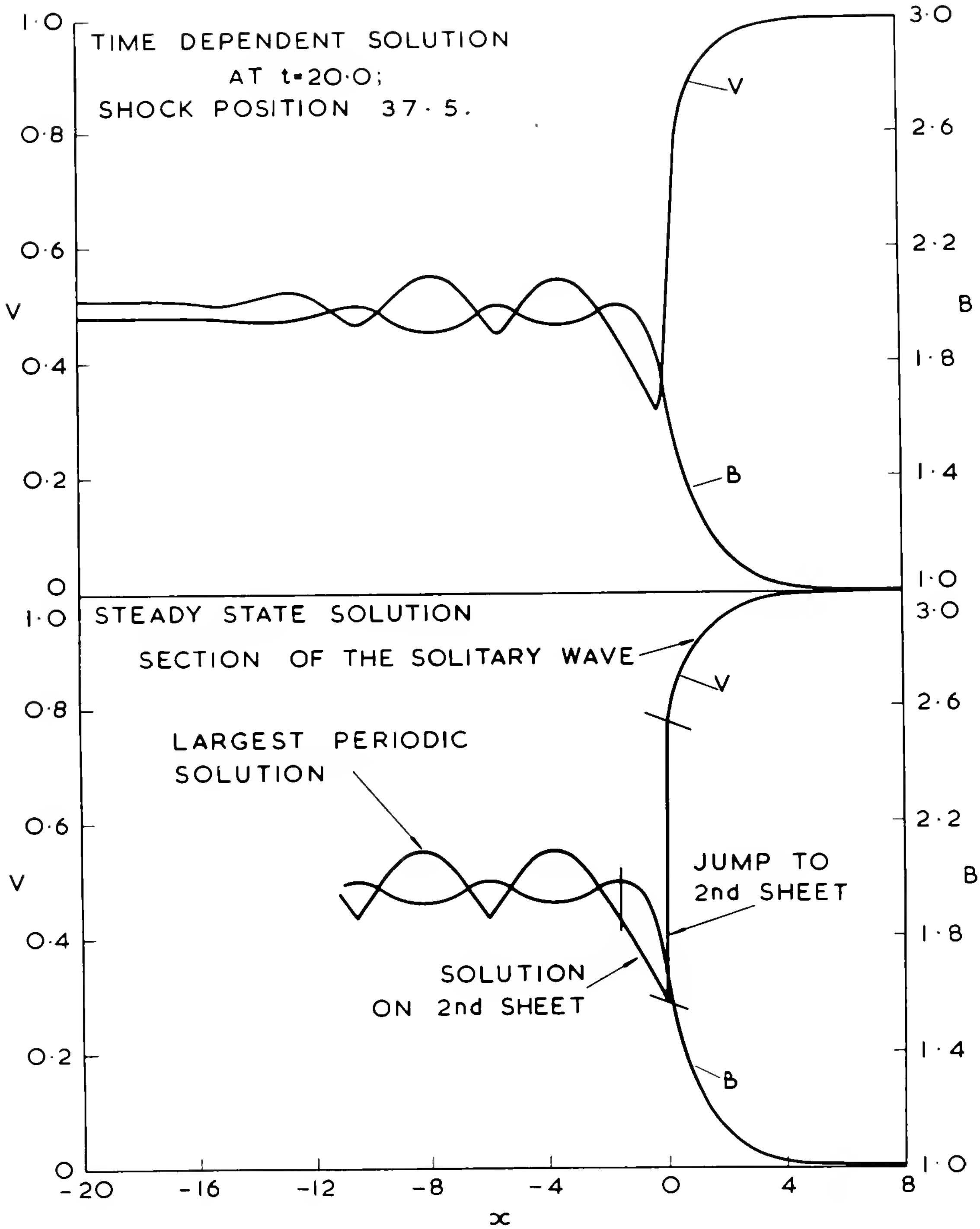

FIG. 6. COMPARISON OF THE TIME DEPENDENT SOLUTION AND A COMPOSITE STEADY STATE SOLUTION FOR CASE IV

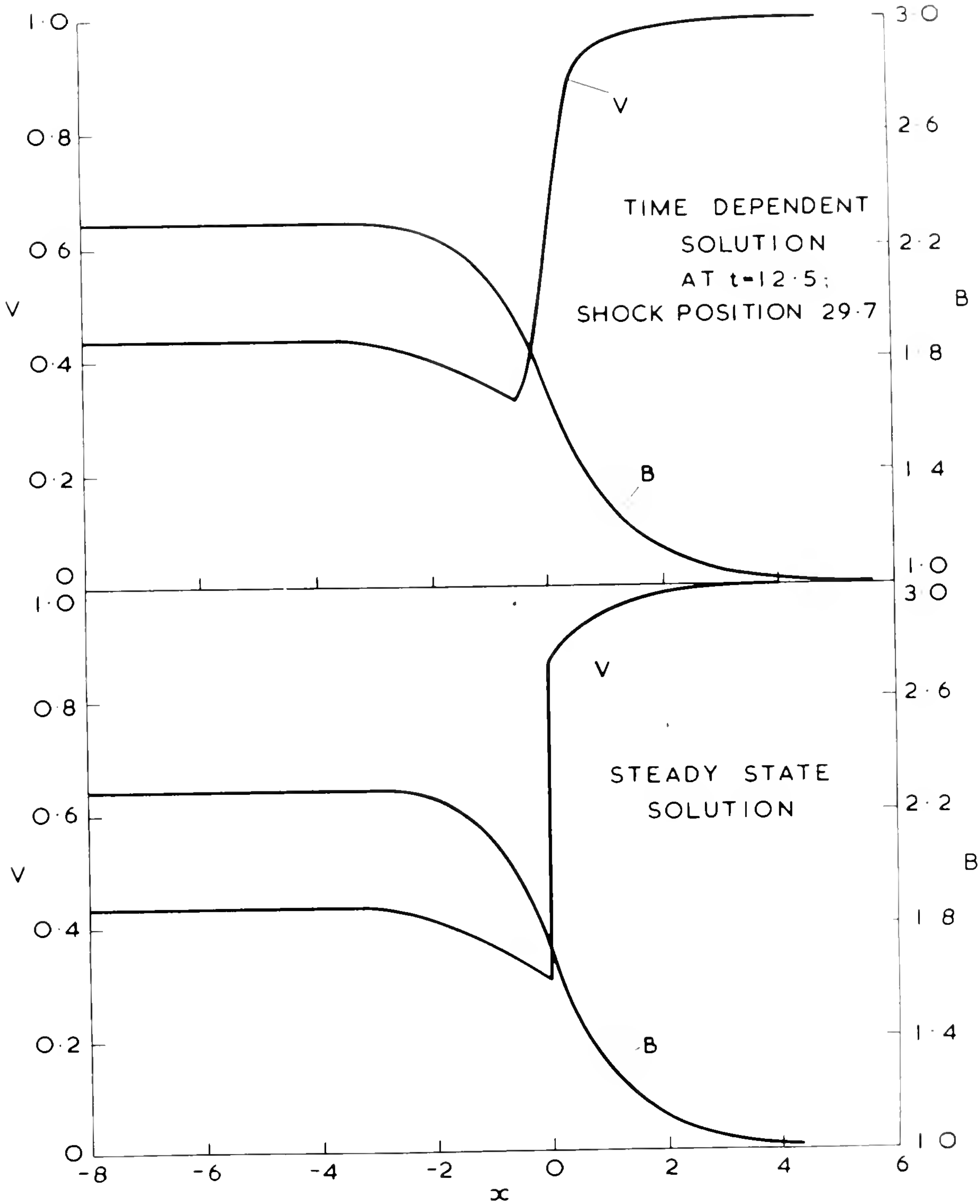

FIG. 7. COMPARISON OF THE TIME DEPENDENT AND STEADY STATE SOLUTIONS FOR CASE V

JUN 6 — 1973

N. Y. U. Institute of
Mathematical Sciences
4 Washington Place
New York 3, N. Y.